

## ESTIMATING ABOVEGROUND CARBON OF TEAK-BASED AGROFORESTRY SYSTEMS IN SABAH, MALAYSIA USING AIRBORNE LiDAR

DANIEL JAMES<sup>1</sup>, NORMAH AWANG BESAR<sup>1</sup>, MAZLIN MOKHTAR<sup>2</sup> AND MUI-HOW PHUA<sup>1\*</sup>

<sup>1</sup>Faculty of Tropical Forestry, Universiti Malaysia Sabah, Jalan UMS, 88400, Kota Kinabalu, Sabah, Malaysia. <sup>2</sup>Institutes of Environment and Development (LESTARI), Universiti Kebangsaan Malaysia, 43600, Bangi, Selangor, Malaysia.

\*Corresponding author: pmh@ums.edu.my

Submitted final draft: 13 July 2021

Accepted: 7 September 2021

<http://doi.org/10.46754/jssm.2022.03.008>

**Abstract:** As a sustainable land use system, agroforestry can potentially mitigate climate change mitigation by sequestering carbon and reducing greenhouse gasses (GHGs) emissions. Since the implementation of the Kyoto Protocol, agroforestry has been recognized as a GHGs mitigation strategy that requires accurate estimation of the carbon storage. Focusing on teak-based agroforestry systems in Sabah, Malaysia, this study examined the use of airborne Light Detection and Ranging (LiDAR) data for aboveground carbon (AGC) estimation. Field inventory data were collected at the agroforestry systems with different intercropping crops to calculate the field AGC. We derived height and canopy density metrics from the LiDAR data to correlate and regress with the field AGC. Stepwise multiple linear regression analyses resulted in a multivariate model that explains 88% of the AGC variance in the agroforestry systems. With the 25<sup>th</sup> and 55<sup>th</sup> height percentiles as predictors, the model had a cross-validated root-mean-square error (RMSEcv) of 6.12 Mg C ha<sup>-1</sup> (Relative RMSEcv: 13.45%). As teak is one of the major plantation species in Southeast Asia, accurate LiDAR-based AGC estimation could assist in developing teak-based agroforestry systems for climate change mitigation in the region.

Keywords: Aboveground biomass, agroforestry systems, airborne laser scanning, Borneo.

### Introduction

An accelerated increase in the concentration of greenhouse gasses, especially carbon emissions in the atmosphere, is of global concern. Unprecedented deforestation and forest degradation activities are among the main contributors to the increasing carbon emissions (MacDicken *et al.*, 2016). Natural forest ecosystems are capable of capturing and storing carbon as biomass in their above and below ground components (Malhi *et al.*, 2008). However, large tracts of forests continue to disappear at an alarming rate around the world especially in the tropical region. Halting deforestation has been a huge challenge largely due to unsustainable forestry and agricultural activities. It is reported that 90% of deforestation is driven by agriculture activities in which 60% are attributed to the extension of agro-industrial farming while the remaining deforestation is a result of small-scale and subsistence cultivation (Laporte *et al.*, 2007).

Ideally, large-scale reforestation to increase forest cover could contribute to stabilization of CO<sub>2</sub> concentration in the atmosphere. However, implementation of this strategy requires large land area, which is also needed for food production (FAO, 2010). As deforested areas are permanently converted for agricultural use, the most conceivable land-use strategy for climate-change mitigation is perhaps to reduce the pressure on natural forest through a sustainable consumptive use strategy, such as the adoption of carbon-rich agroforestry systems (Kumar & Nair, 2011). In comparison to monoculture plantation, the agroforestry systems have a better potential in terms of carbon storage capability in the agriculture-dominated landscapes (Nair *et al.*, 2009). It introduces a more diversified crop planting system on the same unit of land, thus increasing carbon storage efficiency above and below ground (Udawatta & Jose, 2012). The planting of trees, especially timber species, is the

main component that increases the carbon stock density in the agroforestry system (Sharro & Ismail, 2004). Timber trees store higher carbon stock than annual crop or pasture. Nevertheless, the annual crops cultivated also increases the carbon storage of the agroforestry system (Kürsten, 2000).

Agroforestry is recognized as a GHGs mitigation strategy, either as an afforestation or reforestation activity in the Kyoto Protocol under the United Nations Framework Convention on Climate Change (UNFCCC) (Albrecht & Kandji, 2003; Takimoto *et al.*, 2008). The “Reducing Emissions from Deforestation and forest Degradation-plus (REDD+)” is a payment scheme for promoting forest conservation under the UNFCCC. The REDD+ also recognizes the role of agroforestry in climate change mitigation, mainly because of the contribution of planted trees in carbon sequestration (Minang *et al.*, 2014). Estimation of AGC in agroforestry systems is crucial to understanding its potential in carbon storage (Malhi *et al.*, 2008). As an incentive-based strategy, it is imperative to accurately determine the contribution of carbon storage of the agroforestry systems. However, accurate quantitative data on the contributions of different combinations of agroforestry systems in climate change mitigation are seriously lacking (Labata *et al.*, 2012).

The most accurate method to estimate AGC is to cut down the trees, oven-dry them and weigh the dry matter. However, this direct method in assessing AGC stock is prohibitively expensive, destructive and very time consuming (Hunt, 2009). Field based inventory and measurements offers a minimal solution to destructive sampling, in which field measurements are extrapolated to aboveground biomass (AGB) and AGC values using allometric equations (Besar *et al.*, 2020). It is still ineffective in terms of cost and time, especially when it involves carbon stock estimation over a relatively large area (Hyypä *et al.*, 2000).

Remote sensing coupled with field inventory data is a cost-effective approach to estimate the AGB of a relatively large area (Stern, 2007).

The remote sensing is increasingly applied to forest AGC estimation at various spatial scales by extracting the structural information (Le Toan *et al.*, 2004). Forest structural information in high-resolution plays a crucial role in estimating AGB and AGC of mixed vegetation types, including agroforestry plantations (Chen *et al.*, 2015). Many studies examine the use of high-resolution satellite imagery for AGB or AGC estimation (e.g., Patenaude *et al.*, 2005; Muukkonen & Heiskanen, 2007). Although high-resolution optical imagery can be used to estimate diameter at breast height of trees (Phua *et al.*, 2017), tree height, an important determinant of AGB or AGC, cannot be derived from these optical remote-sensing methods.

Airborne Light Detection and Ranging (LiDAR) has emerged as a promising remote-sensing technology to accurately estimate forest AGB and AGC (Patenaude *et al.*, 2005; Van Leeuwen & Nieuwenhuis, 2010). LiDAR emits laser pulses that penetrate tree canopies to detect vegetation vertical structure and enable the extraction of ground elevation, which can be used to derive various canopy height variables. These variables are significantly correlated with field AGB (Chen *et al.*, 2015; Loh *et al.*, 2020). There is an increasing number of studies that use airborne LiDAR data for estimating AGB or AGC in boreal (e.g., Naesset, 2002, 2004), temperate (e.g., Lim & Treitz, 2004; Hollaus *et al.*, 2007) and tropical forests (e.g., Ioki *et al.*, 2014; Phua *et al.*, 2016; Coomes *et al.*, 2017).

Although airborne LiDAR offers high-resolution vegetation structural information, the use of this technology for quantifying AGB or AGC in agroforestry systems has been lacking (Chen *et al.*, 2015; Wang *et al.*, 2016). The high cost of LiDAR data acquisition could be prohibitive to AGC estimation at plantation-scale in developing countries. However, this situation may change in near future because LiDAR sensors integrated into unmanned aerial systems are becoming increasingly available (Torresan *et al.*, 2018). AGB of a diverse agroforestry system in the Amazon is estimated using airborne LiDAR data with an area-based approach (Chen *et al.*, 2015). Separating

monoculture systems from polyculture systems improves AGB estimation in an agroforestry system in the Amazon using LiDAR data. Species identification using hyperspectral data allows AGB estimation in an agroforestry system in Northwest China using airborne LiDAR data (Wang *et al.*, 2016). To the extent of our knowledge, LiDAR-based AGC estimation study in agroforestry systems is absent in Southeast Asia. As teak is one of the main plantation species in the region, we examined the use of airborne LiDAR to estimate AGC of a teak-based agroforestry plantation in Sabah, Malaysia. We first developed AGC estimation

models for the teak-based agroforestry systems using the LiDAR data. We then mapped the AGC of the agroforestry systems using the best model and discussed the LiDAR-based AGC estimation for agroforestry plantations.

**Materials and Methods**

**Study Site**

Balung River Plantation (04° 26' 23" N, 118° 2' 31" E) is in the southern part of Sabah, approximately 40 km north-east of Tawau City (Figure 1). The study area is warm and moist all year-round, a typical tropical climate.

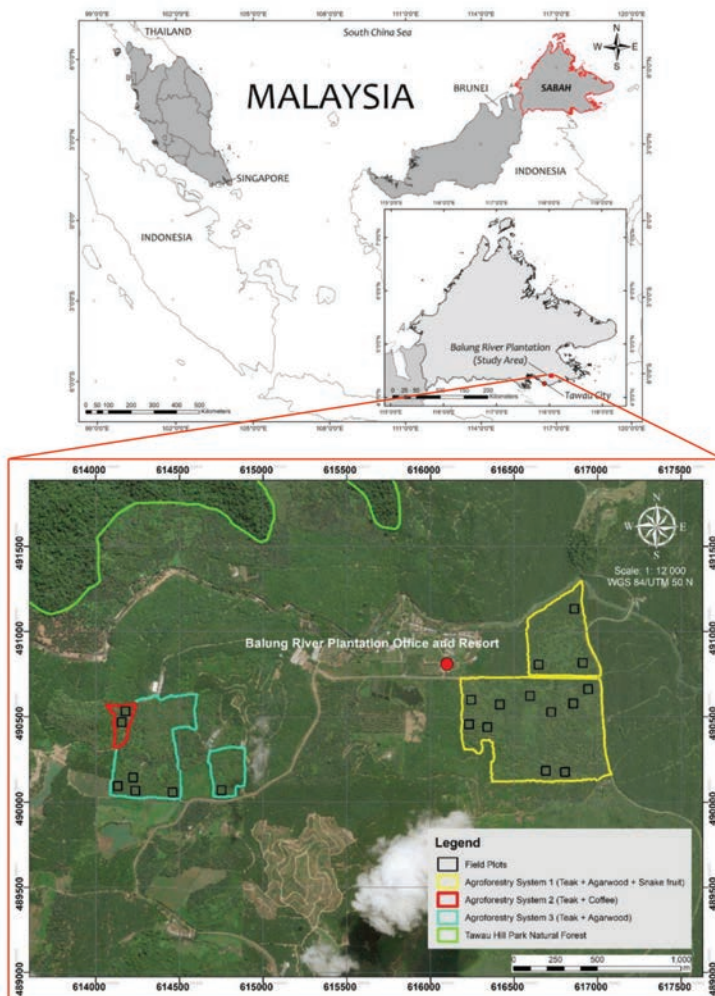


Figure 1: Location of the study area (plot locations are shown with black squares)

Temperature of the study area ranges between 24°C and 33°C, while annual rainfall of up to 2,500 mm per year has been recorded for this area. The topography is generally undulating to hilly with an elevation above 300 m above sea level (a.s.l.). The highest peak nearby the study area is Bald Hill at 468 m a.s.l., in the southwestern part of the plantation area. The soil of Balung River Plantation is of volcanic origin. The bed rocks consist of basalt and andesite (Soehady & Musta, 2012).

Balung River Plantation is owned and managed by Kebun Rimau Sdn. Bhd., a family-run plantation since 1979. The plantation is relatively small, covering an area of approximately 1500 hectares. Balung River Plantation has several planting systems, including monoculture, mixed, intercropping and agroforestry systems. The agroforestry system was introduced in 1993 where timber tree species, such as teak (*Tectona grandis*) and agarwood (*Aquilaria malaccensis*), are planted in combination with snake fruit (*Salacca zalacca*), coffee (*Coffea liberica*) and oil palm (*Elaeis guineensis*). In this study, three teak-based agroforestry systems were examined in terms of its capability to store carbon. Each of these agroforestry combinations was planted in the same year. There are three teak-based agroforestry combinations in the Balung River Plantation, 1. Teak (18 years old) mixed with agarwood (8 years old) and snake fruit (8 years old); 2. Teak (17 years old) mixed with coffee (14 years old) and 3. Teak (18 years old) mixed with agarwood (8 years old).

### Field Data Collection

Field inventory was carried out in the three teak-based agroforestry combinations in the Balung River Plantation in 2014. The three teak-based agroforestry systems were established about the same time and relatively small in area. We established 20 square plots (50 m × 50 m) in the plantations with a stratified random sampling strategy. To avoid over-sampling for the agroforestry system 2, we only established two plots in the smallest plantation (2 ha),

representing 25% of the plantation area. Plot locations were determined using a differential Global Navigation Satellite System (GNSS) receiver (Javad Triumph-1, San Jose, CA, USA), which was placed at the plot's center to record the satellite signals. Post-processing technique was applied to determine the accurate plot locations. Within each plot, tree height and diameter at breast height (DBH) were measured for all teak, coffee and agarwood trees while only height was measured for snake fruit as only height is used in the allometry to calculate AGB for palm species (Frangi & Lugo, 1985).

The measured structural variables were used to calculate field AGB. The field AGB of tree and palm were calculated using following allometric equations:

$$\text{Teak } (T. \textit{grandis}) \text{ AGB} = 0.045 \times (\text{DBH}^2\text{H})^{0.921} \text{ (Ounban et al., 2016) (1)}$$

$$\text{Agarwood } (A. \textit{malaccensis}) \text{ AGB} = 0.1043 \times \text{DBH}^{2.6} \text{ (Hairiah \& Rahayu, 2007) (2)}$$

$$\text{Snake Fruit } (S. \textit{zalacca}) \text{ AGB} = 10 + 6.4 \times \text{H} \text{ (Frangi \& Lugo, 1985) (3)}$$

$$\text{Coffee } (C. \textit{liberica}) \text{ AGB} = 0.281 \times \text{DBH}^{2.06} \text{ (Ketterings et al., 2001) (4)}$$

The field AGB was then converted to field AGC stock using a conversion factor of 0.50 as the carbon content of biomass is about 50% (Houghton & Hackler, 2000). The field AGC within each plot was then summed and divided by the plot size to express the estimated AGC as mega gram carbon per hectare (Mg C ha<sup>-1</sup>).

### Airborne LiDAR Data Acquisition

Airborne LiDAR data was acquired on 9 October 2013 using the Optech Orion-C200, an integrated system of laser sensors coupled with a DGNSS receiver and inertial measurement unit. The system was mounted on a Nomad N22C aircraft that collected the LiDAR data with a scan angle of ±20° and a point repetition frequency of 175 kHz from an altitude of about 500 m above ground (Table 1). Seven flight lines were scanned to cover the agroforestry plantation systems during the data acquisition.



We established a base station with the DGNSS receiver at a surveying benchmark approximately 10 km from the study site for calibrating the LiDAR data. A small area of Tawau City, which is less than 30 km from the study area, was also scanned for calibration of the LiDAR data.

The LiDAR data was calibrated and corrected for boresight misalignments using Optech’s LiDAR Mapping Suit (LMS). The LiDAR point clouds were further processed in Microstation V8i software for noise removal. The processed data had an average point density of 25 point/m<sup>2</sup> and a root-mean-square-error (RMSE) of 0.054 m for z value. The point clouds were classified to ground and non-ground points. The ground points were triangulated using the natural neighbor algorithm to generate a digital terrain model (DTM) in ArcGIS software. The DTM was then used to normalize the non-ground (vegetation) points to absolute heights that represent the canopy heights.

The normalized vegetation points were extracted to calculate various LiDAR metrics. The LiDAR metrics are divided into two types: i) Height metrics, and ii) Canopy cover density (CCD) metrics. The height metrics related to the statistical height distributions including mean height ( $h_{mean}$ ), maximum height ( $h_{max}$ ), 15<sup>th</sup> to 99<sup>th</sup> percentiles ( $h_{15}, h_{20}, h_{25}, \dots, h_{99}$ ), and coefficient of variation of heights ( $h_{cv}$ ). The

CCD is a metric that represents canopy cover, density and permeability for different vertical canopy portions (USDA, 2014). The CCD is a ratio of the number of points of all returns above a specific cut-off height to the total number of points from all returns. We calculated two sets of CCD metrics based on 0.5 m ( $CCD_{>0.5m}$ ) and mean height ( $CCD_{>mean\ height}$ ) as cut-off height values. Statistical analyses were carried out to examine the correlations between these metrics and AGC; and to generate an AGC estimation model for the agroforestry systems.

**Statistical Analysis**

This study aims to develop an AGC estimation model that is applicable to all three agroforestry systems. Firstly, the correlations between field AGB and the LiDAR metrics were examined using Pearson’s correlation coefficient ( $r$ ). Then, we used simple linear regression analysis to develop a single-variable model for LiDAR metric that was strongly correlated with field AGC. Coefficient of determination ( $R^2$ ) and RMSE were used to determine the best model in the simple regression analysis.

Stepwise multiple linear regression was then used to further examine the development of a multivariate AGC estimation model for the agroforestry systems. In the regression analyses, natural-log transformation of the variables

Table 1: LiDAR data acquisition characteristics

Parameter	Details
Date	9 October 2013
System	Optech Orion-C200
Aircraft	Nomad N22C
Laser Wavelength	1541 nm
Flight Altitude	500 m
Flight Speed	90 kts (46.3 m/s)
Scan Angle	±20°
Scan Frequency	50 Hz
Point Per Square Meter (PPM <sup>2</sup> )	8.00
Point Repetitive Frequency (PRF)	175 kHz

was also conducted because canopy heights are known to have nonlinear relationship with structural variables such as AGB and DBH (Yamakura *et al.*, 1986). Multicollinearity effect in the multiple linear regression was determined based on variance inflation factor (VIF) using Statistical Package for the Social Sciences (SPSS) software. A VIF value of 5 was used as tolerance cut-off value to eliminate LiDAR metrics for the multiple linear regression analyses. The best fitting model was assessed and selected based on the Akaike Information Criterion (AIC) value, adjusted coefficient of determination ( $R^2_{adj}$ ), RMSE and RMSE of leave-one-out cross-validation ( $RMSE_{LOOCV}$ ). Cross-validation is preferred for model validation to reduce overfitting and provide unbiased error estimates (Jachowski *et al.*, 2013). For the model generated using natural log-transformed variables, the results were inverted or back transformed to the unit of original values that give a nonlinear model equation. As the natural-log transformation introduces a systematic bias into the RMSE calculations, a correction factor (CF) was applied to the predicted values from the model (Sprugel, 1983).

$$CF = \text{Exp} (SEE/2) \quad (5)$$

where:

CF = Correction factor

SEE = Standard error of the estimate

## Results

### Characteristics of the Agroforestry Systems

Field measurements of the main structural variables such as DBH, H and tree density

were examined to understand the characteristics of the agroforestry systems. Table 2 shows the summary of the field data. Although the planting age and spacing are different among the agroforestry systems, the mean DBH and height values in the three agroforestry systems show no obvious differences. Planted in the same year but with larger spacing, the mean DBH of teak trees in the agroforestry system 1 was about 2 cm smaller than the agroforestry system 3. These teak trees were taller than those in agroforestry system 3 in terms of mean height (+1.68 m). For the same planting spacing but 1 year younger, the teak trees in the agroforestry system 2 were much smaller (-6.42 cm) and shorter (-4.6 m) than the trees in the agroforestry system 3. The mean field AGC calculated from the allometries were 37.34 Mg C ha<sup>-1</sup>, 37.75 Mg C ha<sup>-1</sup> and 69.94 Mg C ha<sup>-1</sup>, for agroforestry system 1, 2 and 3 respectively.

### Correlations between LiDAR Metrics and Field AGC

There were nine LiDAR height metrics that were strongly correlated ( $r > 0.75$ ) with field AGC (Table 3). All the height metrics were positively correlated with the field AGC except the metric of  $h_{cv}$ , which was negatively correlated with the field AGC. With an  $r$  of 0.923,  $h_{25}$  had the strongest correlation with the AGC. This was followed by  $h_{35}$  ( $r$ : 0.887) and  $h_{cv}$  ( $r$ : -0.882). On the other hand, none of the CCD metrics showed a strong correlation with the field AGC.

Table 2: Field data summary

System	Average	Maximum	Minimum	S.D.	S.E.
Agroforestry System 1					
<i>Teak (18 years old)</i>					
<i>Tree Density (trees/ha)</i>	89.00	124.00	48.00	19.42	5.39
<i>DBH (cm)</i>	34.96	49.30	16.80	6.23	0.37
<i>Height (m)</i>	21.97	28.50	13.70	2.50	0.15
<i>Field AGC (Mg C ha<sup>-1</sup>)</i>	25.07	43.11	16.08	7.01	1.95

<i>Snake Fruit (8 years old)</i>					
<i>Tree Density (trees/ha)</i>	657.00	900.00	524.00	111.35	30.88
<i>Height (m)</i>	3.24	5.50	1.00	0.57	0.01
<i>Field AGC (Mg C ha<sup>-1</sup>)</i>	10.09	13.72	7.94	1.68	0.47
<i>Agarwood (8 years old)</i>					
<i>Tree Density (trees/ha)</i>	71.00	104.00	44.00	20.75	5.76
<i>DBH (cm)</i>	9.80	29.40	1.50	4.96	0.33
<i>Height (m)</i>	6.00	10.40	1.50	1.66	0.11
<i>Field AGC (Mg C ha<sup>-1</sup>)</i>	2.18	7.93	0.36	2.06	0.57
<b><i>Overall Field AGC (Mg C ha<sup>-1</sup>)</i></b>	<b>37.34</b>	<b>53.15</b>	<b>25.80</b>	<b>7.53</b>	<b>2.09</b>
<i>Agroforestry System 2</i>					
<i>Teak (17 years old)</i>					
<i>Tree Density (trees/ha)</i>	174.00	184.00	164.00	14.14	10.00
<i>DBH (cm)</i>	30.46	50.90	9.30	7.34	0.79
<i>Height (m)</i>	15.69	24.30	6.90	3.68	0.39
<i>Field AGC (Mg C ha<sup>-1</sup>)</i>	28.83	32.17	25.48	4.73	3.35
<i>Coffee (14 years old)</i>					
<i>Tree Density (trees/ha)</i>	1144.00	1284.00	1004.00	197.99	140.00
<i>DBH (cm)</i>	6.65	13.00	0.50	2.23	0.09
<i>Height (m)</i>	2.95	9.60	1.30	0.70	0.03
<i>Field AGC (Mg C ha<sup>-1</sup>)</i>	8.92	32.17	25.48	4.62	3.27
<b><i>Overall Field AGC (Mg C ha<sup>-1</sup>)</i></b>	<b>37.75</b>	<b>37.82</b>	<b>37.66</b>	<b>0.11</b>	<b>0.08</b>
<i>Agroforestry System 3</i>					
<i>Teak (18 years old)</i>					
<i>Tree Density (trees/ha)</i>	199.00	252.00	140.00	41.90	18.74
<i>DBH (cm)</i>	36.88	63.00	21.30	7.00	0.44
<i>Height (m)</i>	20.29	26.70	11.20	2.44	0.16
<i>Field AGC (Mg C ha<sup>-1</sup>)</i>	57.84	64.88	49.99	5.60	2.50
<i>Agarwood (8 years old)</i>					
<i>Tree Density (trees/ha)</i>	244	304	112	77.97	34.87
<i>DBH (cm)</i>	12.79	26.50	2.80	4.46	0.26
<i>Height (m)</i>	7.99	19.90	2.50	3.09	0.18
<i>Field AGC (Mg C ha<sup>-1</sup>)</i>	12.10	19.17	5.52	5.18	2.32
<b><i>Overall Field AGC (Mg C ha<sup>-1</sup>)</i></b>	<b>69.94</b>	<b>79.35</b>	<b>63.88</b>	<b>5.76</b>	<b>2.58</b>

Note: S.D. = Standard Deviation; S.E. = Standard Error

Table 3: Correlations between LiDAR metrics and field AGC ( $r > 0.75$ )

Metrics	<i>r</i> value
$h_{15}$	*0.761
$h_{20}$	*0.846
$h_{25}$	*0.923
$h_{30}$	*0.854
$h_{35}$	*0.887
$h_{40}$	*0.830
$h_{45}$	*0.812
$h_{mean}$	*0.842
$h_{cv}$	*-0.882

\*Significant at the 0.001 level

### Regression Analysis

Table 4 summarizes the results of simple linear regression and multiple linear regression analyses. Model 1 was the best model with highest  $R^2$  for the simple regression analysis ( $R^2 = 0.86$ ; AIC = 132.45). The independent variable

of the best model was  $h_{25}$  metric. For original variables, the  $h_{25}$  and  $h_{55}$  were selected as the independent variables in the stepwise regression analyses (Model 2:  $R^2_{adj} = 0.88$ ; AIC = 129.49). However, transforming the independent or dependent or both with natural-log did not improve the model's adjusted  $R^2$ . In fact, the stepwise regression analysis with natural-log transformed metrics as independent variables resulted in a single-variable model with the lowest  $R^2$  (Model 3:  $R^2_{adj} = 0.77$ ; AIC = 142.27).

Figure 2 shows the scatterplots between field AGC and LiDAR estimated AGC for all four models. As expected, the model 3 with  $\text{Ln}(h_{cv})$  as predictor had the highest  $\text{RMSE}_{cv}$  (8.07 Mg C ha<sup>-1</sup>). The model 2 with the highest  $R^2_{adj}$  had the lowest  $\text{RMSE}_{cv}$  (7.11 Mg C ha<sup>-1</sup>). Moreover, its relative  $\text{RMSE}_{cv}$  was only 13.45% of the average AGC, lowest among the models. Therefore, the model 2 was selected as the best model for estimating AGC of the teak-based agroforestry systems.

Table 4: Summary of the AGC estimation models using the LiDAR metrics

Model	Dependent Variable	Independent Variables	$R^2$ / Adjusted $R^2$	AIC	RMSE (Relative RMSE)	RMSE <sub>cv</sub> (Relative RMSE <sub>cv</sub> )
1	AGC	$h_{25}$	0.86	132.45	5.71 Mg C ha <sup>-1</sup> (12.54%)	6.52 Mg C ha <sup>-1</sup> (14.34%)
2	AGC	$h_{25}$ $h_{55}$	0.88	129.49	5.04 Mg C ha <sup>-1</sup> (11.08%)	6.12 Mg C ha <sup>-1</sup> (13.45%)
3	AGC	$\text{Ln}(h_{cv})$	0.77	142.27	7.30 Mg C ha <sup>-1</sup> (16.03%)	8.07 Mg C ha <sup>-1</sup> (17.72%)
4	$\text{Ln}(\text{AGC})$	$h_{25}$ $h_{55}$	0.85	-83.98	5.79 Mg C ha <sup>-1</sup> (12.71%)	7.11 Mg C ha <sup>-1</sup> (15.62%)
5	$\text{Ln}(\text{AGC})$	$\text{Ln}(h_{25})$	0.79	-74.09	6.42 Mg C ha <sup>-1</sup> (14.15%)	7.11 Mg C ha <sup>-1</sup> (15.61%)



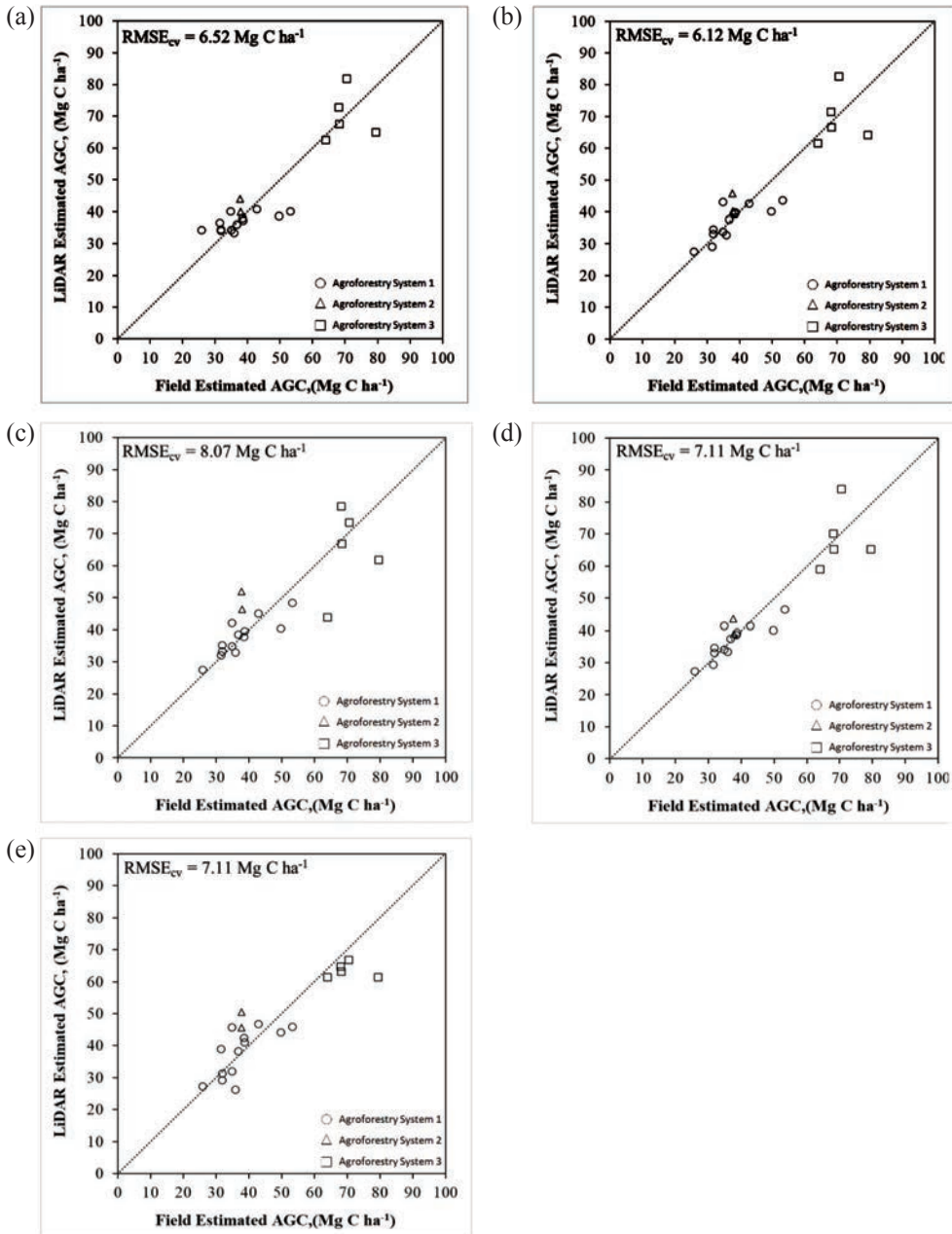


Figure 2: Field AGC ( $\text{Mg C ha}^{-1}$ ) versus LiDAR estimated AGC ( $\text{Mg C ha}^{-1}$ ) of the regression models; (a) model 1, (b) model 2, (c) model 3, (d) model 4, (e) model 5

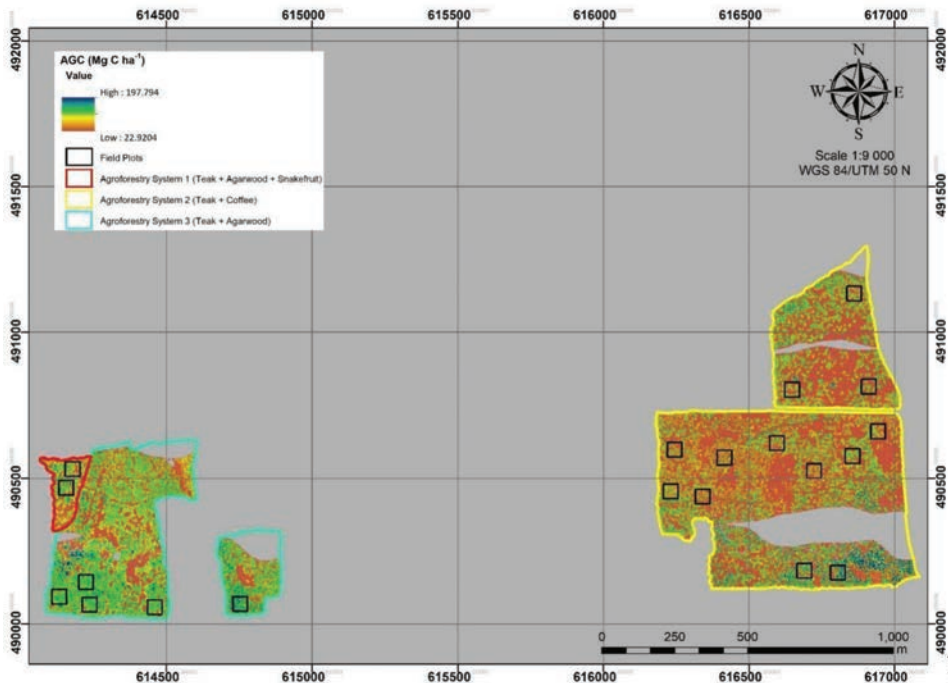


Figure 3: AGC distribution in the plantation at 1 m resolution produced using the Model 2. The missing data area in the polyculture systems 1 and 3 were gaps between flight lines due to weather conditions during the data acquisition

## Discussion

Different types of agroforestry systems have different carbon storage capability, ranging between 0.29 and 15.21 Mg C ha<sup>-1</sup> yr<sup>-1</sup> (Nair *et al.*, 2009; Jose & Bardhan, 2012). In a mixed or intercropped plantation system, timber species often contribute more than 50 percent of the total carbon stock (Weidne *et al.*, 2011). Compared to smaller trees or crops planted as understory crops, timber species can store much higher amounts of carbon. Our results are in agreement with exiting studies; AGC of timber trees was much higher than the understory tree or crop species. In this study, teak trees at the upperstory canopy accounted for 77% of the overall AGC in the three agroforestry systems. In contrast, the understory species only contributed to 23% of the overall AGC. Agarwood and coffee trees constituted 10% and 6% of the overall AGC of the agroforestry systems, while snake fruit crop contributed 7% of the overall field AGC.

AGC of teak trees at different growth stages ranges from 18.13 Mg C ha<sup>-1</sup> at year 5 to 181.13 Mg C ha<sup>-1</sup> at year 50 (Sreejesh *et al.*, 2013). Although the planting age of the teak trees in the study area is not very different, the teak AGC in the three systems ranged between 25.07 Mg C ha<sup>-1</sup> and 57.84 Mg C ha<sup>-1</sup>. The AGC of teak trees was 67%, 73% and 83% of the overall AGC for the agroforestry systems 1, 2 and 3 respectively. The AGC variations were at least partially due to the planting density effect. At about 200 trees/ha, the teak trees accumulated the highest AGC (57.84 Mg C ha<sup>-1</sup>) for the agroforestry system 3. At a lower planting density of 174 tree/ha, AGC of the agroforestry system 2 was about 50% lower than the agroforestry system 3. However, planting density did not show a substantial effect on AGC of the agroforestry system 1, which has a much lower planting density of 89 trees/ha. As this indicates possible spatial variations due to other site factors, it would be better to predict the AGC distributions over the

plantation areas using high-precision remote sensing technologies.

Accurate AGC estimation is a prerequisite of an incentive-based climate change mitigation system. We examined the use of LiDAR data to develop an AGC estimation model for teak-based agroforestry systems. LiDAR's canopy heights are known to strongly correlate with mean forest canopy height (Lagomasino *et al.*, 2016; Loh *et al.*, 2020). Based on the correlation analysis, there were nine height metrics showing strong correlations with field AGC of the agroforestry systems ( $r > 0.75$ ). In contrast, none of the CCD metrics strongly correlated with the field AGC. Since height is one of the main structural variables in an AGB allometry (Yamakura *et al.*, 1986), the results highlighted the potential of height metrics in AGC estimation of the teak-based agroforestry systems.

LiDAR-derived height metrics can explain forest canopy structure variations and well correlated with AGB or AGC (Ioki *et al.*, 2014; Loh *et al.*, 2020). With height metrics as predictors, the resulting regression models were able to explain 79% to 88% of the AGC variances for the agroforestry systems. Our results are in the similar range of a LiDAR-based AGC estimation study in an agroforestry system in the Brazilian Amazon (Chen *et al.*, 2015). The best estimation model was a multivariate model with  $h_{25}$  and  $h_{55}$  as predictors, which explained 88% of the field AGC variance. The  $h_{25}$ , a relatively low percentile height metric, was included in all regression models except the model 3, highlighting the influence of height distributions of understory vegetation in the AGC estimation. The role of height metrics of lower percentiles has been observed in other studies that use LiDAR data to estimate AGC in both planted and natural forests (Stephens *et al.*, 2007; d'Oliveira *et al.*, 2012; Lim & Treitz, 2004). Height metrics of lower percentiles show strong relationships with AGC in a planted forest in New Zealand (Stephens *et al.*, 2007). In a boreal forest, Lim and Trietz (2004) reported that the use of 25<sup>th</sup> height percentile improves the AGB estimation

model. These studies suggest that height metrics at lower percentiles contain both tree height and canopy density information. In our study, dense canopies of snake fruit and coffee trees at the understory layers in the agroforestry systems 1 and 2 influenced the point cloud distributions in the lower percentiles especially at heights ranging from 0.5 to 5 meters. High-density point clouds in these understory vegetations indicate that the upperstory teak layer is relatively open. The inclusion of a height metric at higher percentile (55<sup>th</sup> height percentile) only marginally improved the best estimation model in this study. In the Brazilian Amazon, height metrics of upper percentiles (80<sup>th</sup> and 90<sup>th</sup> height percentiles) are predictors of AGB of the agroforestry systems (Chen *et al.*, 2015). Differences in the selection of LiDAR metrics in AGC modeling could be explained by the differences in site conditions including the variety of species planted (Chen, 2013).

Tree-crop combinations in an agroforestry system can be quite diverse as in the case of Chen *et al.* (2015). Beside monoculture systems, the agroforestry systems consist of various fruits and timber species. Separating monoculture from polyculture systems significantly improves the AGC estimation model's  $R^2$  from 0.38 to 0.75, while the RMSE<sub>cv</sub> is reduced from 56.40 Mg C ha<sup>-1</sup> to 35.9 Mg C ha<sup>-1</sup> (Chen *et al.*, 2015). Classifying monoculture and polyculture systems using a high-resolution RapidEye satellite imagery allows the implementation of the estimation model. In Northwest China, hyperspectral imagery was used to identify the timber species in the agroforestry system and to facilitate tree AGB estimation using LiDAR data (Wang *et al.*, 2016). As the study only involved a few species, it would be premature to conclude that the approach is effective in identifying multiple mixed timber species planted in an agroforestry system. The potential of airborne multispectral or hyperspectral imagery in retrieving tree and crop for accurate LiDAR-based AGC estimation deserves further investigation in future.

## Conclusion

Agroforestry systems are a sustainable consumptive use system that could contribute to climate change mitigation. In a teak-based agroforestry plantation in Sabah, Malaysia, we found that spatial variations in field AGC were unexplained by age and planting density. We examined the use of airborne LiDAR data to model and map the spatial distribution of the AGC. LiDAR-based AGC models resulted in this study explained 77% to 88% of field AGC variance. The best model with 25<sup>th</sup> and 55<sup>th</sup> percentile metrics as predictors had a relatively low cross-validated RMSE of 13.45%. For teak-based agroforestry plantations such as in Malaysia, as well as other parts of Southeast Asia, fitting AGC of different teak-based agroforestry systems to one universal model is desirable for AGC estimation at plantation scale. Since LiDAR sensors integrated into unmanned aerial systems (UAV) are becoming increasingly available, the LiDAR based AGC estimation will be instrumental in supporting agroforestry for climate change mitigation activities in the region.

## Acknowledgements

This study was funded by the Ministry of Higher Education of Malaysia (Grant no: FRGS/1/2019/WAB07/UMS/01/1 and RACE/F1/STWN2/UMS/6). We sincerely thank Tan Sri Datuk Seri Panglima Harris Mohd. Salleh (Balung River Plantation owner) and Mr. Samalih Kupsa (Balung River Plantation Manager) for permission to conduct the research in the plantation.

## References

- Albretch, A., & Kandji, S. (2003). Carbon sequestration in tropical agroforestry systems. *Agriculture, Ecosystems and Environment*, 99(1), 15-27.
- Besar, N. A., Suardi, H., Phua, M. H., James, D., Mokhtar, M. B., & Ahmed, M. F. (2020). Carbon stock and sequestration potential of an agroforestry system in Sabah, Malaysia. *Forests*, 11(2), 210.
- Chen, Q. (2013). LiDAR remote sensing of vegetation biomass. In Q, Weng & G, Wang (Eds.), *Remote sensing of natural resources* (pp. 399-420). Boca Raton: CRC Press.
- Chen, Q., Lu, D., Keller, M., dos-Santos, M. N., Bolfe, E. L., Feng, Y., & Wang, C. (2015). Modeling and mapping agroforestry aboveground biomass in the Brazilian Amazon using Airborne Lidar Data. *Remote Sensing*, 8(1), 21.
- Coomes, D. A., Dalponte, M., Jucker, T., Asner, G. P., Banin, L. F., Burslem, D. F., Lewis, S. L., Nilus, R., Phillips, O. L., Phua, M.-H., & Qie, L. (2017). Area-based vs tree-centric approaches to mapping forest carbon in Southeast Asian forests from airborne laser scanning data. *Remote Sensing of Environment*, 194, 77-88.
- d'Oliveira, M. V., Reutebuch, S. E., McGaughey, R. J., & Andersen, H. E. (2012). Estimating forest biomass and identifying low-intensity logging areas using airborne scanning lidar in Antimary State Forest, Acre State, Western Brazilian Amazon. *Remote Sensing of Environment*, 124, 479-491.
- FAO. (2010). *Global forest resources assessment 2010*. Rome: FAO.
- Frangi, J. L., & Lugo, A. E. (1985). Ecosystem dynamics of a subtropical floodplain forest. *Ecological Monographs*, 55(3), 351-369.
- Hairiah, K., & Rahayu, S. (2007). *Pengukuran karbon tersimpan di berbagai macam penggunaan lahan*. Bogor: World Agroforestry Centre.
- Hollaus, M., Wagner, W., Maier, B., & Schadauer, K. (2007). Airborne laser scanning of forest stem volume in a mountainous environment. *Sensors*, 7(8), 1559-1577.
- Houghton, R. A., & Hackler, J. L. (2000). Changes in terrestrial carbon storage in the United States: The roles of agriculture and forestry. *Global Ecology and Biogeography*, 9(2), 125-144.

- Hunt, C. A. (2009). *Carbon sinks and climate change: Forests in the fight against global warming*. Cheltenham, UK: Edward Elgar Publishing.
- Hyypä, J., Hyypä, H., Inkinen, M., Engdahl, M., Linko, S., & Zhu, Y. H. (2000). Accuracy comparison of various remote sensing data sources in the retrieval of forest stand attributes. *Forest Ecology and Management*, 128(1), 109-120.
- Ioki, K., Tsuyuki, S., Hirata, Y., Phua, M. H., Wong, W. V. C., Ling, Z. Y., Saito, H., & Takao, G. (2014). Estimating above-ground biomass of tropical rainforest of different degradation levels in Northern Borneo using airborne LiDAR. *Forest Ecology and Management*, 328, 335-341.
- Jachowski, N. R., Quak, M. S., Friess, D. A., Duangnamon, D., Webb, E. L., & Ziegler, A. D. (2013). Mangrove biomass estimation in Southwest Thailand using machine learning. *Applied Geography*, 45, 311-321.
- Jose, S., & Bardhan, S. (2012). Agroforestry for biomass production and carbon sequestration: An overview. *Agroforestry Systems*, 86(2), 105-111.
- Ketterings, Q. M., Coe, R., van Noordwijk, M., & Palm, C. A. (2001). Reducing uncertainty in the use of allometric biomass equations for predicting aboveground tree biomass in mixed secondary forests. *Forest Ecology and Management*, 146(1), 199-209.
- Kumar, B. M., & Nair, P. R. (2011). *Carbon sequestration potential of agroforestry systems: Opportunities and challenges*. Netherlands: Springer.
- Kürsten, E. (2000). Fuelwood production in agroforestry systems for sustainable land use and CO<sub>2</sub>-mitigation. *Ecological Engineering*, 16, 69-72.
- Labata, M. M., Aranico, E. C., Tabaranza, A. C. E., Patricio, J. H. P., & Amparado Jr, R. F. (2012). Carbon stock assessment of three selected agroforestry systems in Bukidnon, Philippines. *Advances in Environmental Sciences*, 4(1), 5-11.
- Lagomasino, D., Fatoyinbo, T., Lee, S., Feliciano, E., Trettin, C., & Simard, M. (2016). A comparison of mangrove canopy height using multiple independent measurements from land, air, and space. *Remote Sensing*, 8(4), 327.
- Laporte, N. T., Stabach, J. A., Grosch, R., Lin, T. S., & Goetz, S. J. (2007). Expansion of industrial logging in Central Africa. *Science*, 316(5830), 1451-1451.
- Le Toan, T., Quegan, S., Woodward, I., Lomas, M., Delbart, N., & Picard, G. (2004). Relating radar remote sensing of biomass to modelling of forest carbon budgets. *Climatic Change*, 67(2-3), 379-402.
- Lim, K. S., & Treitz, P. M. (2004). Estimation of above ground forest biomass from airborne discrete return laser scanner data using canopy-based quantile estimators. *Scandinavian Journal of Forest Research*, 19(6), 558-570.
- Loh, H. Y., James, D., Ioki, K., Wong, W. V. C., Tsuyuki, S., & Phua, M.-H. (2020). Aboveground biomass changes in Tropical Montane Forest of Northern Borneo estimated using Spaceborne and Airborne Digital Elevation Data. *Remote Sensing*, 12(22), 3677.
- MacDicken, K., Jonsson, Ö., Piña, L., Maulo, S., Adikari, Y., Garzuglia, M., Lindquist, E., Reams, G., & D'Annunzio, R. (2016). *The global forest resources assessment 2015* (2nd ed.). Rome: FAO.
- Malhi, Y., Roberts, J. T., Betts, R. A., Killeen, T. J., Li, W., & Nobre, C. A. (2008). Climate change, deforestation, and the fate of the Amazon. *Science*, 319(5860), 169-172.
- Minang, P. A., Van Noordwijk, M., Duguma, L. A., Alemagi, D., Do, T. H., Bernard, F., Agung, P., Robiglio, V., Catacutan, D., Suyanto, S., Armas, A., Aguad, C. S., Feudjio, M., Galudra, G., Maryani, R., White, D., Widayati, A., Kahurani, E.,



- Namirembe, S., Leimona, B., & Armas, A. (2014). REDD+ Readiness progress across countries: Time for reconsideration. *Climate Policy*, 14(6), 685-708.
- Weidne, S., Bünner, N., Casillano, Z. L., Sales-Come, R., Erhardt, J., Frommberg, P., Peuse, F., & Ringhof, E. (2011). *Towards sustainable land-use: A socio-economic and environmental appraisal of agroforestry systems in the Philippines*. Berlin: Humboldt-Universität zu Berlin.
- Muukkonen, P., & Heiskanen, J. (2007). Biomass estimation over a large area based on standwise forest inventory data and ASTER and MODIS satellite data: A possibility to verify carbon inventories. *Remote Sensing of Environment*, 107(4), 617-624.
- Næsset, E. (2002). Predicting forest stand characteristics with airborne scanning laser using a practical two-stage procedure and field data. *Remote Sensing of Environment*, 80(1), 88-99.
- Næsset, E. (2004). Practical large-scale forest stand inventory using a small-footprint airborne scanning laser. *Scandinavian Journal of Forest Research*, 19(2), 164-179.
- Nair, P. R., Kumar, B. M., & Nair, V. D. (2009). Agroforestry as a strategy for carbon sequestration. *Journal of Plant Nutrition and Soil Science*, 172(1), 10-23.
- Ounban, W., Puangchit, L., & Diloksumpun, S. (2016). Development of general biomass allometric equations for *Tectona grandis* Linn. f. and *Eucalyptus camaldulensis* Dehnh. plantations in Thailand. *Agriculture and Natural Resources*, 50(1), 48-53.
- Patenaude, G., Milne, R., & Dawson, T. P. (2005). Synthesis of remote sensing approaches for forest carbon estimation: Reporting to the Kyoto Protocol. *Environmental Science and Policy*, 8(2), 161-178.
- Phua, M. H., Hue, S. W., Ioki, K., Hashim, M., Bidin, K., Musta, B., Suleiman, M., Yap, S. W., & Maycock, C. R. (2016). Estimating logged-over lowland rainforest aboveground biomass in Sabah, Malaysia using airborne LiDAR data. *Terrestrial, Atmospheric and Oceanic Sciences*, 27(4), 481-489.
- Phua, M. H., Ling, Z. Y., Coomes, D. A., Wong, W., Korom, A., Tsuyuki, S., Ioki, K., Hirata, Y., Saito, H., & Takao, G. (2017). Seeing trees from space: Above-ground biomass estimates of intact and degraded montane rainforests from high-resolution optical imagery. *iForest*, 10(3), 625-634.
- Sharrow, S. H., & Ismail, S. (2004). Carbon and nitrogen storage in agroforests, tree plantations, and pastures in western Oregon, USA. *Agroforestry Systems*, 60(2), 123-130.
- Soehady, H. F. W., & Musta, B. (2012). Effect of micro-fabrics on uniaxial strength of weathered volcanic rocks from Tawau, Sabah. *Borneo Science*, 30, 14-23.
- Sprugel, D. G. (1983). Correcting for bias in log-transformed allometric equations. *Ecology*, 64(1), 209-210.
- Sreejesh, K. K., Thomas, T. P., Rugmini, P., Prasanth, K. M., & Kripa, P. K. (2013). Carbon sequestration Potential of Teak (*Tectona grandis*) plantations in Kerala. *Research Journal of Recent Sciences*, 2, 167-170.
- Stephens, P. R., Watt, P. J., Loubser, D., Haywood, A., & Kimberley, M. O. (2007). Estimation of carbon stocks in New Zealand planted forests using airborne scanning LiDAR. *International Archives of the Photogrammetry, Remote Sensing and Spatial Information Sciences*, 36, 389-394.
- Stern, N. (2007). *The economics of climate change: The stern review*. Cambridge: Cambridge University Press.
- Takimoto, A., Nair, P. R., & Nair, V. D. (2008). Carbon stock and sequestration potential of traditional and improved agroforestry systems in the West African Sahel. *Agriculture, Ecosystems and Environment*, 125(1), 159-166.

- Udawatta, R. P., & Jose, S. (2012). Agroforestry strategies to sequester carbon in temperate North America. *Agroforestry Systems*, 86(2), 225-242.
- United States Department of Agriculture. (2014). *First order LiDAR metrics: A supporting document for LiDAR deliverables*. Salt Lake City, Utah: USDA.
- Van Leeuwen, M., & Nieuwenhuis, M. (2010). Retrieval of forest structural parameters using LiDAR remote sensing. *European Journal of Forest Research*, 129(4) 749-770.
- Wang, Z., Liu, L., Peng, D., Liu, X., Zhang, S., & Wang, Y. (2016). Estimating woody aboveground biomass in an area of agroforestry using airborne light detection and ranging and compact airborne spectrographic imager hyperspectral data: individual tree analysis incorporating tree species information. *Journal of Applied Remote Sensing*, 10(3), 036007.
- Yamakura, T., Hagihara, A., Sukardjo, S., & Ogawa, H. (1986). Aboveground biomass of tropical rain forest stands in Indonesian Borneo. *Vegetatio*, 68(2), 71-82.